Heritage Science

RESEARCH

Open Access

FTIR study on the phase transition of experimental and archaeological burnt ivory

Kai Wang[1], Yuhang He[1], Ruiqi Shao[1], Hao Zhao[1], Honglin Ran[2], Yu Lei[2] and Yihang Zhou[1*]

Abstract

Recent excavation of the elephant ivories at the Sanxingdui site of the Shang Dynasty in Sichuan, China brings attention to the burnt features of the ivories. However, burnt ivories cannot be assessed by the same criteria established for burnt bones because of the differences in the ways that the two materials respond to heat. This study examines differences in the phase transition characteristics of ivory and bone, and confirms that the threshold temperature of the alteration in ivories is lower than that in bones. In our analysis, elephant ivories and bovine bones burnt at the temperatures between 200 and 1000 °C in oxidizing or reducing atmosphere are prepared and comparatively investigated by attenuated total reflection Fourier transform infrared spectroscopy. The results show that the transformation from magnesium-substituted hydroxyapatite (Mg-HAp) to magnesium-substituted β-tricalcium phosphate in ivory dentin takes place at the temperature as low as 800 °C, while β-tricalcium phosphate is not observed in bovine bones burnt at 1000 °C or below mainly because of the different magnesium contents. Due to the destruction of Mg-HAp at 800 °C in ivories, cyanamidapatite that could form in bones burnt under reducing atmosphere is absent in burnt ivories. With reference to the experimental burnt ivories, archaeological burnt ivories from the Sanxingdui site can now be clearly determined to be burnt unevenly at temperatures up to around 800 °C. This study may provide further information for archaeological research on ivories from the Sanxingdui site and identification of burnt bioapatite materials in other archaeological findings.

Keywords: Archaeological burnt ivories, Phase transition, Hydroxyapatite, β-Tricalcium phosphate, Fourier transform infrared spectroscopy, Sanxingdui site

Introduction

Osseous materials (bone, tooth, antler, ivory, and artifacts made from them) are a major component of many archaeological assemblages, and provide information on environment, subsistence, technology, and culture. Alteration of osseous materials by intentional or unintentional burning can bring changes in color [1–3], fracture patterns [3–5], crystallinity [2, 6–8], etc. that provide additional information on the use of fire. For instance, the ongoing excavation of the K3 to K8 sacrificial pits of the Sanxingdui site in Guanghan City, Sichuan, China has found piles of elephant ivories along with delicate bronzewares. Radiocarbon dating of the K4 pit is 3148–2966 cal. BP [9] in the late period of the Shang Dynasty. Some of the ivories show evidences of burning, which might have been intentional (religious or ceremonial) or unintentional. References related to interpreting heat treatment of ivory are very limited and mainly focused on the coloration and weight [10–13]. However, the coloration of archaeological ivories can be also affected by metal ions from complex burial environment and by the burning atmosphere, which makes these subjective methods less precise and requires more caution.

Ivory is a generic term, which describes the material obtained from predominantly exo-skeletal incisor teeth or tusk of several animal species: elephant, mammoth, walrus, hippopotamus, whales, etc. [14]. But here ivory

*Correspondence: zhouyihang@pku.edu.cn

[1] School of Archaeology and Museology, Peking University, Beijing 100871, China
Full list of author information is available at the end of the article

refers to the elephant tusk, mainly consist of dentin with cementum at the periphery [15]. As a osseous material, the ivory is also composed of carbonated hydroxyapatite and collagen, but with increased Mg content [14]. Unlike bones, studies have found that whitlockite was formed after thermal treatment of mammoth tusk from 600 to 1000 °C [16] and β-tricalcium phosphate (TCP) can be formed in human teeth at temperatures as low as 750 °C [17], while the appearance of TCP from bones appears to be sporadic and occur at temperatures around 1100 °C [18]. Because of the similarities between ivories and mammoth tusks or human teeth in high magnesium content in dentin, the phase transition is suspected to take place in burnt ivories, which would serve as a solid indication of burning apart from other less reliable features like colors and fractures. Therefore, to provide a reference for the archaeological burnt ivories and deepen our knowledge of the cause of different responses to burning between ivories and common osseous materials like bones, Fourier transform infrared spectroscopy as a micro-invasive, convenient, and informative analytical technique is adopted to investigate the experimental burnt ivories in comparison to bovine bones and prepared apatite samples. The acquired data and understandings are then served as references to determine the ivory samples from the Sanxingdui site.

Materials and methods

Samples

Cleaned compact tissue of bovine femur was purchased from markets and segmented into $10 \times 5 \times 3$ mm blocks. The ivory dentin was disassembled from an artwork of 1980s in a shape of $10 \times 3 \times 1$ mm flat sticks. Three burnt ivory samples containing both dentin and cementum were collected from the K8 pit of the Sanxingdui site of the Bronze age in Sichuan Province, China.

Preparation of hydroxyapatite (HAp), magnesium substituted hydroxyapatite (Mg-HAp) and carbonated hydroxyapatite (CHAp)

The HAp, Mg-HAp and CHAp were prepared with reference to [19] with some modifications. 9.93 g (42.1 mmol) $Ca(NO_3)_2{\cdot}4H_2O$ was dissolved in 50 ml deionized water with addition of 0.1 ml 25% ammonia and heated to 50 °C. 3.30 g (25.0 mmol) $(NH_4)_2HPO_4$ was dissolved in 100 ml deionized water with addition of 10 ml 25% ammonia. The above phosphate solution was added dropwise to the calcium solution with vigorous magnetic stirring. The mixed solution was then stirred for 30 min at 50 °C and filtered under reduced pressure. The resulted hydroxyapatite precipitate was washed by 100 ml deionized water and subsequently 100 ml ethanol and dried under reduced pressure.

For preparing carbonated CHAp, the phosphate solution contained 3.23 g (24.5 mmol) $(NH_4)_2HPO_4$ and 53 mg (0.5 mmol) Na_2CO_3. For preparing Mg-HAp, the calcium solution contained 8.44 g (35.8 mmol) $Ca(NO_3)_2{\cdot}4H_2O$ and 1.28 g (6.3 mmol) $MgCl_2{\cdot}4H_2O$ and was heated to 80 °C. The rest procedures are the same as above.

Preparation of burnt bones and ivories

The burnt bovine bones and ivories (dentin) were prepared by heating raw bones and ivories at 200, 400, 600, 800, and 1000 °C respectively for 2 h in an electric tube furnace in either oxidizing or reducing atmosphere. For oxidizing atmosphere, the sample was directly exposed to the air. For reducing atmosphere, the samples were buried in the charcoal/quartz powder mixture to simulate the reducing conditions that could occur in ancient times. The prepared HAp, Mg-HAp and CHAp were burnt at 600, 800, and 1000 °C respectively in oxidizing atmosphere for reference.

Hydrothermal transformation

To distinguish the phase transition caused by burning from burial, the prepared HAp and Mg-HAp were also treated by the hydrothermal treatment. Specifically, 0.20 g prepared HAp or Mg-HAp was treated in 80 ml 0.05 mol/l pH 5.0 acetate buffer, pH 5.8 acetate buffer, pH 7.0 Tris buffer, and pH 8.0 Tris buffer respectively at 95 °C for 2d. The prepared samples of HAp and Mg-HAp were used in place of bone and ivory samples for the following reasons. First, the decomposed organics during the hydrothermal treatment would probably result in uncontrolled pH. Second, to simulate the phase transition during the burial, an elevated temperature is a must to accelerate the process but too high temperatures should be also avoided as higher temperatures are more likely to deviate from the burial environment. The prepared HAp and Mg-HAp were similar to decayed bones and ivories without organics in compositions, but in low crystallinity and more reactive, whose phase transitions would probably take place at a lower temperature and in shorter time.

Attenuated total reflection Fourier transform infrared spectroscopy (ATR-FTIR)

Grinded samples were analyzed by attenuated total reflection Fourier transform infrared spectroscopy (Nicolet IS5) with a range from 4000 to 400 cm^{-1} under 4 cm^{-1} resolution. Each spectrum was the result of an average of 16 scans. The spectra were processed by advanced ATR calibration in Omnic 9 software using the parameters as diamond, 45° incident angle, 1.0 reflection times and 1.62 refractive index. The infrared split factor (IRSF) is

adopted to determine the crystallinity of hydroxyapatite by measuring the heights at the absorption bands at 565 and 605 cm^{-1} and the height of the minimum trough between the split peaks and the higher IRSF values indicate larger crystal sizes and more regularly organized lattice [7, 20].

X-ray diffraction (XRD)

XRD analysis was performed on OLYMPUS Terra with Co anode Kα ray to identify the phase in the grinded sample when necessary. The working voltage of X-ray tube was 30 kV. The working electric current was 300 μA. The scanning degree 2θ is from 5° to 55° with step size 0.05°, scan step time 10s and accumulation of 32 times.

Results and discussion

Phase changes under heat treatment

The spectra of the raw bovine bone and ivory dentin both (shown in Fig. 1) contain absorption bands of amide I at 1652 cm^{-1}, amide II at 1548 cm^{-1}, $\nu_3(CO_3^{2-})$ at 1454 cm^{-1} and 1414 cm^{-1}, $\nu_3(PO_4^{3-})$ at 1088 cm^{-1} and 1018 cm^{-1}, $\nu_1(PO_4^{3-})$ at 963 cm^{-1}, $\nu_2(CO_3^{2-})$ at 873 cm^{-1}, and $\nu_4(PO_4^{3-})$ at 601 cm^{-1} and 561 cm^{-1}, representing composites of collagen and carbonated hydroxyapatite (CHAp). The main difference between the two materials before burning lie in the C=O stretching vibration band at 1745 cm^{-1} suggesting the presence of lipids in bones and absence in ivories. With the increase of the burning temperatures from 200 to 1000 °C, the absorption bands of organics and CO_3^{2-} of both materials decrease as they decompose, and the IRSF increase shown in Table 1, which suggests the recrystallization process starts at around 600 °C as previously reported [1, 2, 8].

After being burnt at temperatures between 800 and 1000 °C, notable phase changes take place and vary between bones burnt in oxidizing atmosphere and reducing atmosphere, and also between bones and ivories. The

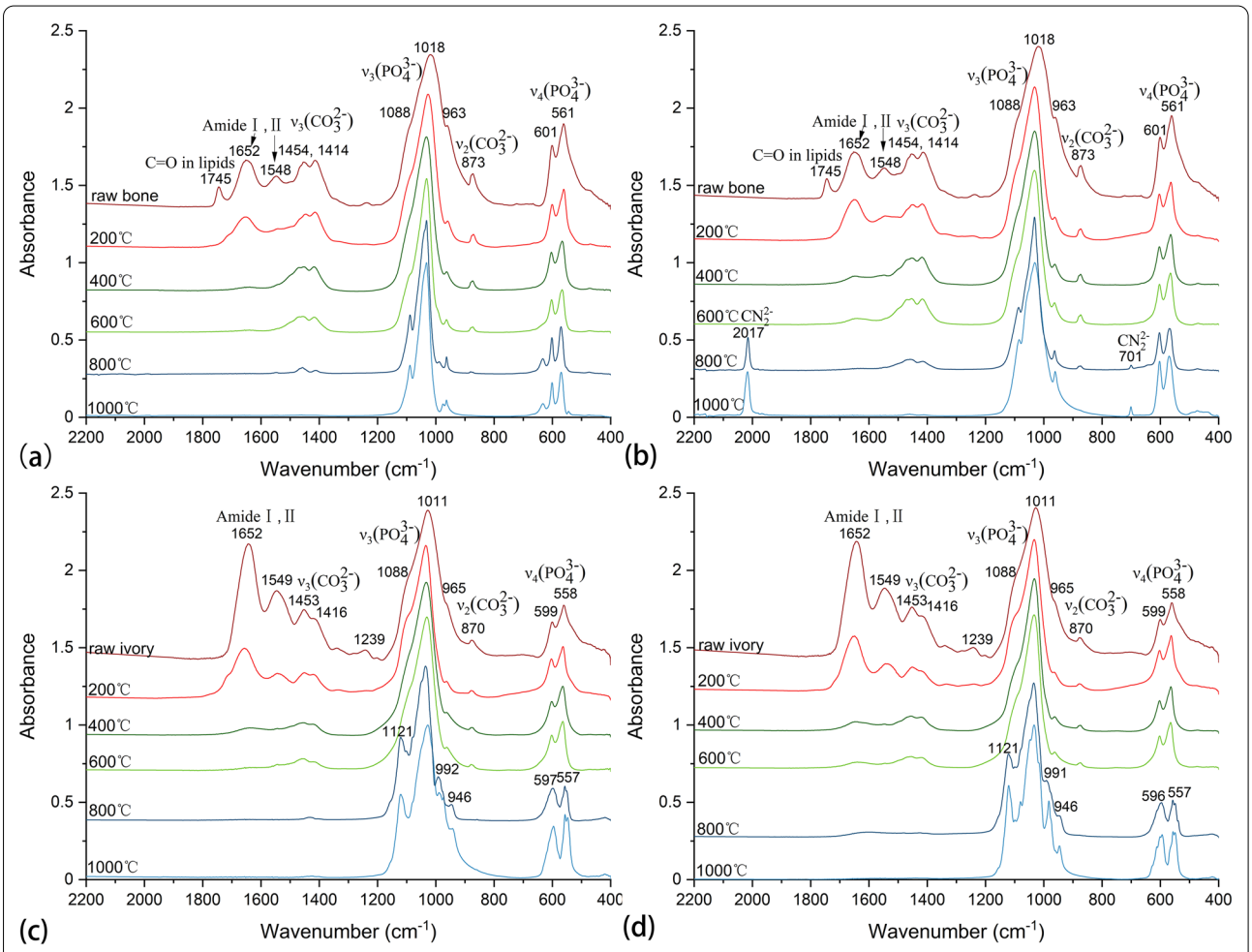

Fig. 1 FTIR spectra of **a** bones burnt under oxidizing atmosphere, **b** bones burnt under reducing atmosphere, **c** ivories burnt under oxidizing atmosphere, **d** ivories burnt under reducing atmosphere

Table 1 IRSFs of the experimental burnt ivories and bones

	Burning atmosphere and temperature	IRSF		Burning atmosphere and temperature	IRSF
Bovine bone	Raw	3.00	Ivory dentin	Raw	2.86
	Oxidizing 200 °C	3.54		Oxidizing 200 °C	3.07
	Oxidizing 400 °C	3.45		Oxidizing 400 °C	2.90
	Oxidizing 600 °C	4.02		Oxidizing 600 °C	4.14
	Oxidizing 800 °C	6.17		Oxidizing 800℃	4.90 (Mg-TCP)
	Oxidizing 1000 °C	5.94		Oxidizing 1000 °C	5.63 (Mg-TCP)
	Reducing 200 °C	3.21		Reducing 200 °C	3.17
	Reducing 400 °C	3.22		Reducing 400 °C	3.41
	Reducing 600 °C	3.67		Reducing 600 °C	3.36
	Reducing 800 °C	4.77 (cyanamidapatite)		Reducing 800 °C	4.55 (Mg-TCP)
	Reducing 1000 °C	4.35 (cyanamidapatite)		Reducing 1000 °C	6.46 (Mg-TCP)

spectra in Fig. 1a show the transformation of CHAp to well-crystallized HAp according to the triplet $\nu_4(PO_4^{3-})$ band [21] and much higher IRSFs of the bones burnt at temperatures between 800 and 1000 °C. The absorption bands at 2017 cm^{-1} and 701 cm^{-1} in Fig. 1b suggest the formation of CN_2^{2-} group and corresponding cyanamidapatite ($Ca_{10}(PO_4)_6CN_2$) [22, 23] in bones burnt at temperatures between 800 and 1000 °C in reducing atmosphere. The replacement of OH^- by CN_2^{2-} may also impede the recrystallization judging by the lower IRSFs of bones burnt at temperatures between 800 and 1000 °C in reducing atmosphere compared to those in oxidizing atmosphere. However, these bands of CN_2^{2-} group are absent in the spectra of ivories burnt in reducing atmosphere (shown in Fig. 1d) as another phase forms. The ivories burnt at temperatures between 800 and 1000 °C show a new FTIR pattern with $\nu_3(PO_4^{3-})$ bands shifting to 1121 cm^{-1}, 1034 cm^{-1}, 992 cm^{-1}, $\nu_1(PO_4^{3-})$ bands shifting to 946 cm^{-1}, and $\nu_4(PO_4^{3-})$ bands shifting to 597 cm^{-1} and 557 cm^{-1}, which match the spectrum of magnesium-substituted β-tricalcium phosphate (Mg-TCP) [24, 25]. The XRD spectra of the ivories burnt at 800 °C (shown in Additional file 1: Fig. S1) also matches well the spectrum of whitlockite $Ca_{18}Mg_2(HPO_4)_2(PO_4)_{12}$ (JCDPS No. 70-2064). However, it is hard to distinguish whitlockite from Mg-TCP with high Mg content by XRD [26]. Although some of the bands such as 992 cm^{-1} fit the characteristic bands of whitlockite [27], the key band of P–O–H stretching in HPO_4^{2-} at 917 cm^{-1} is absent. Accordingly, the phase of the ivories burnt at temperatures between 800 and 1000 °C cannot be determined as whitlockite but Mg-TCP instead. Since the transformation of Mg-HAp to Mg-TCP coincides with the temperature range of CN_2^{2-} formation, CN_2^{2-} group can no longer be kept in the lattice as it does in apatite. Therefore, the burning atmosphere has little influence on ivories unlike bovine bones. It is also noted that the IRSFs drops when new phases such as Mg-TCP or cyanamidapatite are formed at 800 °C, which suggests the burning temperature cannot be solely determined by IRSF.

Many bioapatite materials are known to more easily transform to β-tricalcium phosphate (TCP) or Mg-TCP. For instance, TCP or Mg-TCP was found in fish bones of some species burnt at temperatures as low as 600 °C while samples of mammals and birds did not form this phase at temperatures below 1000 °C [28, 29]. TCP was found in deer antler burnt at temperatures between 800 and 1000 °C while whale tympanic bulla only formed CaO and HAP under the same conditions [30]. Additionally, mammoth tusk was reported to transform from Mg-HAp to whitlockite during thermal treatment from 600 to 1000 °C [16]. Human teeth were also observed the occurrence of TCP at temperatures as low as 750 °C [17]. It is found that the magnesium ion destabilizes the structure of hydroxyapatite, which reduces the temperature of the hydroxyapatite–whitlockite transition as its content increases [31]. As whitlockite shares a very closed XRD pattern with Mg-TCP, the XRD-determined whitlockite is likely to be Mg-TCP as well. Elemental analysis of the raw bone and ivory dentin shows they share a similar (Mg + Ca)/P ratio while the Mg/(Mg + Ca) ratio in the ivory dentin (0.112) is much higher than that in the bone (0.031) (shown in Table 2). FTIR spectra shown in Fig. 2a, b also confirms that the transition of the prepared Mg-HAp to Mg-TCP takes place at a lower temperature (600 °C) compared to that of HAp to TCP (800 °C). Therefore, it is believed that the higher magnesium content in ivories destabilize the HAp lattice, allowing it more easily to transform to the TCP structure. Additionally, when CO_3^{2-} substitution is increased by 2% in HAp, it requires a temperature as high as 1000 °C for CHAp to partially transform to TCP (shown in Fig. 2c). The substitution of

PO_4^{3-} by CO_3^{2-} would cause the (Ca + Mg)/P ratio to deviate more from the theoretical value of TCP (1.5), creating the barrier for the transformation. For the same reason, bovine bones with even higher CO_3^{2-} substitution in HAp cannot form TCP when burnt below 1000 °C.

Distinction from the phase transition during burial

Since magnesium substitution in HAp destabilizes the lattice, Mg-HAp is also suspected to be less stable in burial environments at pH normally from 5.0 to 8.0. As shown in Fig. 3a, the prepared HAp shows identical FTIR spectra after treated at 95 °C and pH from 5.0 to 8.0 for 2d. Mg-HAp, however, is not as stable as HAp at pH 5.0 and shows new $\nu_3(PO_4^{3-})$ bands at 1134 cm^{-1}, 1060 cm^{-1}, 993 cm^{-1}, P–O–H stretching in HPO_4^{2-} at 918 cm^{-1} and $\nu_4(PO_4^{3-})$ bands shifting to 603 cm^{-1} and 560 cm^{-1} (shown in Fig. 3b), which match the spectrum of whitlockite. The XRD spectrum of the Mg-HAp treated at pH 5.0 (shown in Additional file 1: Fig. S2) matches whitlockite as well with reference to JCDPS No. 70-2064. Although the hydrothermal treatment of the prepared HAp and Mg-HAp cannot reproduce the actual burial outcomes of bones and ivories at archaeological sites, it is indicated that ivories are probably less stable

Table 2 Elemental analysis of bones and ivories

	Mg (at%)	Ca (at%)	P (at%)	Mg/(Mg + Ca)	(Mg + Ca)/P
Bovine bone	0.57 ± 0.01	17.96 ± 0.57	9.66 ± 0.21	0.031 ± 0.002	1.92 ± 0.09
Ivory	1.75 ± 0.09	13.88 ± 0.48	8.09 ± 0.22	0.112 ± 0.008	1.93 ± 0.03

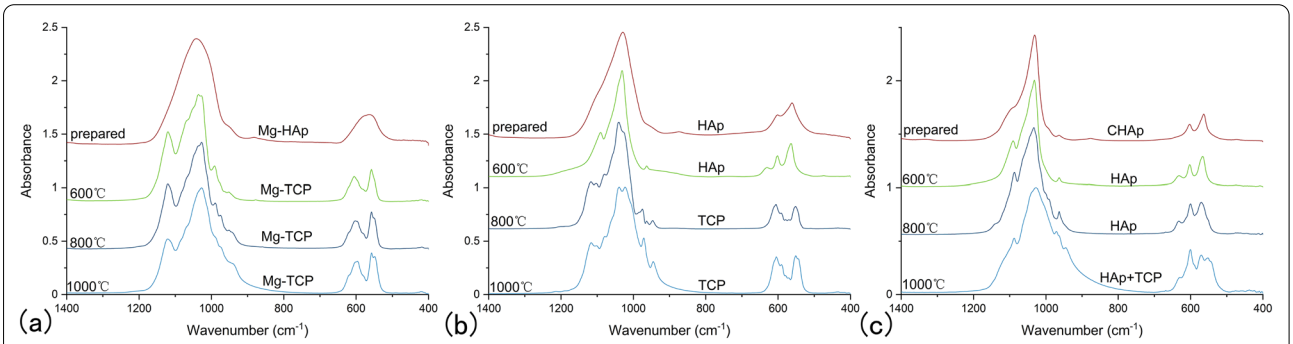

Fig. 2 FTIR spectra of the burnt prepared **a** Mg-HAp, **b** HAp, and **c** CHAp

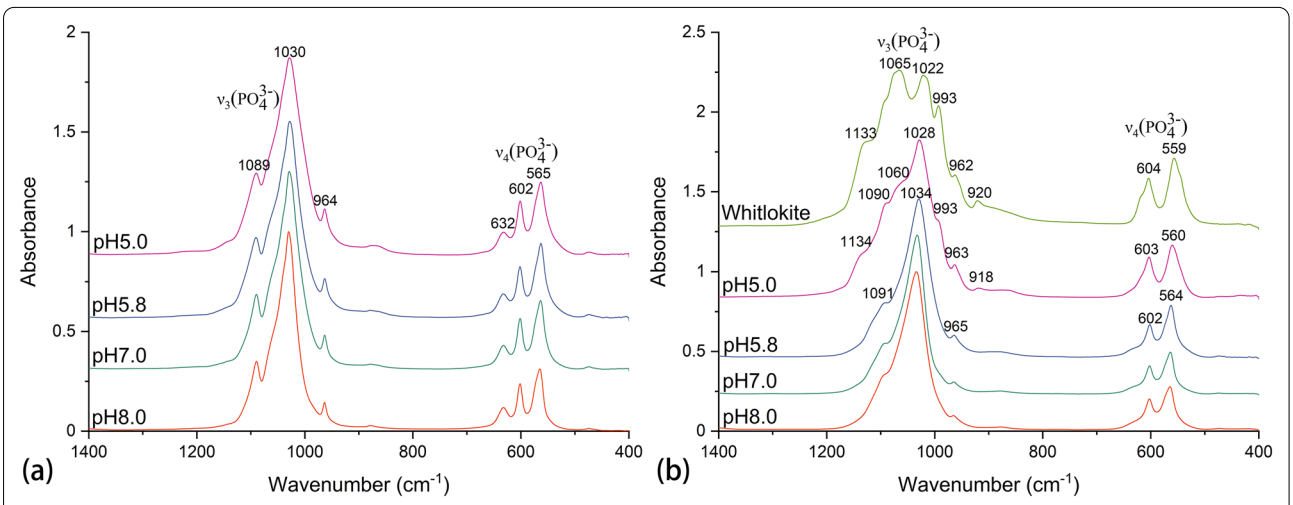

Fig. 3 FTIR spectra of HAp and Mg-HAp treated under different pH conditions

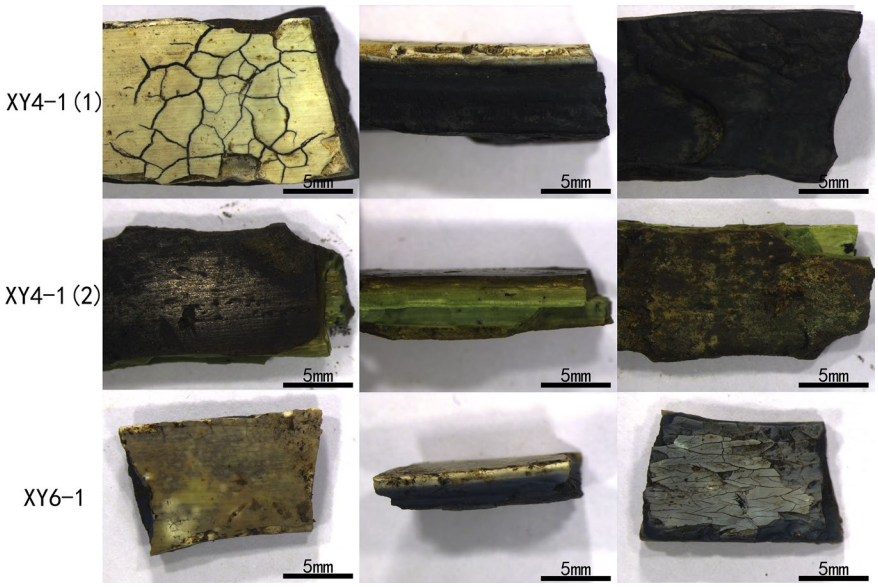

Fig. 4 Appearances of the ivories from the Sanxingdui site

in acidic environment due to the higher Mg content and the phase transition is possible. Supposing whitlockite is formed, it is easily distinguishable from the Mg-TCP of burnt ivories in FTIR spectrum based on the higher wavenumber of $\nu_3(PO_4^{3-})$ band at 1134 cm^{-1} compared to 1121 cm^{-1} in the spectra of Mg-TCP and the presence of HPO_4^{2-} band at around 918 cm^{-1}. Nonetheless, the high content of Mg in ivories dissipates over time, at rates that differ with burial conditions. Elemental analysis of ivory specimens from modern to paleolithic periods found that ivories earlier than 2700 BP have lost the majority of Mg and are indistinguishable from other osseous materials with respect to Mg contents [32–34]. This fact indicates that phase transition of ivories during actual burials may be even harder due to a continuous loss of Mg compounds, making the compositions close to non-substituted HAp. Therefore, the possibility of phase transition of ivories during burials remain to be verified until more archaeological specimens are tested or better burial imitation methodology is established.

Ivory samples from the Sanxingdui site

Shown in Fig. 4, the 3 ivory samples from the Sanxingdui site display different appearances. Both XY4-1(1) and XY6-1 have whitish cementum and black dentin, while XY4-1(2) have black cementum and green dentin stained by Cu^{2+} from bronze rusts, which implies different burning temperatures.

The FTIR spectra of the 3 ivory samples are shown in Fig. 5 and the IRSF are shown in Table 3. Only the spectrum of XY6-1 dentin shows featured absorption bands

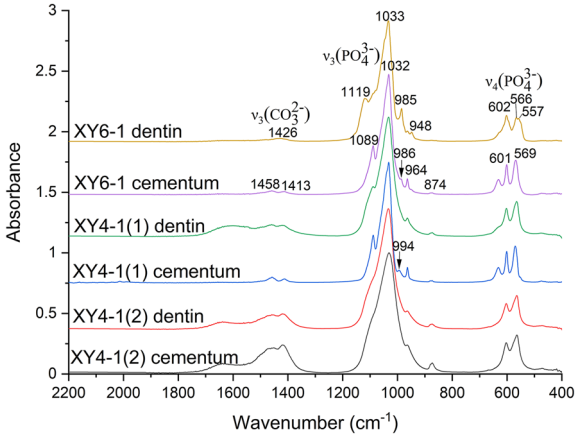

Fig. 5 FTIR spectra of the ivory samples from the Sanxingdui site

Table 3 IRSFs of the ivories from the Sanxingdui site

	IRSF	Inferred burning temperature
XY4-1(1) cementum	7.12	Around 800 °C
XY4-1(1) dentin	4.21	Around 600 °C
XY4-1(2) cementum	3.18	< 600 °C, mildly burnt
XY4-1(2) dentin	3.45	< 600 °C, mildly burnt
XY6-1 cementum	6.07	Around 800 °C
XY6-1 dentin	4.44 (Mg-TCP)	Around 800 °C

of Mg-TCP at 1119 cm^{-1}, 985 cm^{-1}, 948 cm^{-1}, and 557 cm^{-1}, which indicates the transformation of Mg-HAp to Mg-TCP and the burning temperature was presumably

around 800 °C. Both cementum samples of XY6-1 and XY4-1(1) show evident recrystallization of Mg-HAp judging by the high IRSFs over 6 (shown in Table 3) and decreases in the absorption bands of CO_3^{2-} at around 1458 cm^{-1}, 1413 cm^{-1}, and 874 cm^{-1}. With reference to Fig. 1, the burning temperature of them is determined to be also around 800 °C as CO_3^{2-} bands marginally remain. In the spectra of the two samples, the tiny absorption bands at around 990 cm^{-1} indicate the transformation of Mg-HAp to Mg-TCP in cementum was very limited at around 800 °C due to the much lower Mg content in cementum than that in dentin [14]. Because most of the HAp is preserved in cementum, the absence of absorption bands of CN_2^{2-} indicates an oxidizing burning condition. The spectrum of XY4-1(1) dentin and the IRSF as 4.21 matches the features of ivory dentin burnt at around 600 °C. The spectra of both the dentin and cementum of XY4-1(2) show pronounced $\nu_3(CO_3^{2-})$ absorption bands at 1454 cm^{-1} and 1414 cm^{-1}, and the IRSFs lower than 3.5. Considering the light green dentin without carbonized features and black cementum, it was presumably burnt mildly. The slightly increased IRSF should mostly result from collagen decomposition [7].

The FTIR results of the 3 ivory samples from the Sanxingdui site suggests that these ivories were unevenly burnt at temperatures up to around 800 °C. Unlike bones, burnt ivories have nothing to do with cooking food. Ivories may serve as a symbol of power or raw materials for handcrafts. However, the loss of collagen in burnt ivories would cause a dramatic decrease in mechanical strength, making them less durable and processable. Therefore, the unevenly burnt ivories in the Sanxingdui site are possibly evidences for an accidental conflagration or a sacrificial custom.

Conclusion

Despite the similar compositions, the phase transition of ivories is not identical to common bones (e.g. bovine bones) when the burning temperature reaches 800 °C. The transformation from Mg-HAp to Mg-TCP in ivory dentin takes place at the temperature as low as 800 °C, while TCP is not observed in bovine bones burnt at 1000 °C or below. Because of the destruction of HAp structure in ivory dentin at a lower temperature, cyanamidapatite appearing in bones burnt in reducing atmosphere is absent in ivory dentin and thus the burning atmosphere has little influence on the ivory dentin. Experiments on the prepared HAp and Mg-HAp suggests the significance on the magnesium substitution on the phase transition from HAp to TCP and explains the different phases in ivories and bones burnt at 800 °C or above.

On the basis of the FTIR study on the experimental burnt ivories, the burning temperatures of the samples from the Sanxingdui site are determined to be up to around 800 °C and they were burnt unevenly.

The present study highlights the distinction in phase transition in burnt ivories by applying the widely used micro-invasive ATR-FTIR technique, which would provide an important reference for the identification of archaeological burnt ivories.

Supplementary Information

The online version contains supplementary material available at https://doi.org/10.1186/s40494-022-00769-4.

Additional file 1: Figure S1. XRD spectra of burnt ivories at 800 °C in (a) reducing atmosphere, and (b) oxidizing atmosphere. **Figure S2.** XRD spectrum of the prepared Mg-HAp treated at 95 °C, pH 5.0 for 2d.

Acknowledgements
Not applicable.

Author contributions
All the experiments were designed and carried out by KW and YZ. The data were analyzed and discussed by YZ, KW, YH and RS. The samples were collected by YH, RS, and HZ with the help of HR and YL. The manuscript was written by YZ and KW. All authors read and approved the final manuscript.

Funding
Not applicable.

Availability of data and materials
The datasets analyzed during the current study are available from the corresponding author upon reasonable request.

Declarations

Competing interests
There is no financial and non-financial competing interest.

Author details
[1]School of Archaeology and Museology, Peking University, Beijing 100871, China. [2]Sichuan Provincial Cultural Relics and Archaeology Research Institute, Chengdu 610041, Sichuan, China.

Received: 10 June 2022 Accepted: 10 August 2022
Published online: 22 August 2022

References

1. Shipman P, Foster G, Schoeninger M. Burnt bones and teeth: an experimental study of color, morphology, crystal structure and shrinkage. J Archaeol Sci. 1984;11(4):307–25.
2. Stiner MC, Kuhn SL, Weiner S, Bar-Yosef O. Differential burning, recrystallization, and fragmentation of archaeological bone. J Archaeol Sci. 1995;22(2): 223–237.
3. Gre´vin G, Bailet P, Quatrehomme G, Ollier A. Anatomical reconstruction of fragments of burned human bones: a necessary means for forensic identification. Forensic Sci Int. 1998; 96: 129–134.
4. Buikstra JE, Swegle M. Bone modification due to burning: experimental evidence. In: Bonnichsen R, Sorg MH, editors. Peopling of the America's centre for the studies of the first Americans. Orono: Maine; 1989. p. 247–58.
5. Thurman MD, Willmore LJ. A replicative cremation experiment. N Am Archaeol. 1981;2(4): 275–283.

6. Enzo S, Bazzoni M, Mazzarello V, Piga G, Bandiera P, Melis P. A study by thermal treatment and x-ray powder diffraction on burnt fragmented bones from tombs II, IV and IX belonging to the hypogeic necropolis of "Sa Figu" near Ittiri, Sassari (Sardinia, Italy). J Archaeol Sci. 2007;34(10):1731–7.
7. Surovell TA, Stiner MC. Standardizing infra-red measures of bone mineral crystallinity: an experimental approach. J Archaeol Sci. 2001;28: 633–642.
8. Thompson T, Islam M, Bonniere M. A new statistical approach for determining the crystallinity of heat-altered bone mineral from FTIR spectra. J Archaeol Sci. 2013; 40(1): 416–422.
9. Xie C, Xu D, Han Y, et al. AMS radiocarbon dating of K4 sacrificial pit at Sanxingdui site in Guanghan City, Sichuan Province. Sichuan Cult Relics. 2021; 216: 117–120.
10. Baer NS, Indictor N, Frantz JH, Appelbaum B. The effect of high temperature on ivory. Stud Conserv, 1971; 16(1): 1–8.
11. Baer NS, Appelbaum B, Indictor N. The effect of long-term heating on ivory. Bull Am Group Int Inst Conserv Hist Artist Works. 1971;12(1):55–9.
12. Robins GV, Del Re C, Seeley NJ, Davis AG, Hawari JA. A spectroscopic study of the Nimrud ivories. J Archaeol Sci. 1983;10(4):385–95.
13. Reiche I, Vignaud C, Menu M. Heat induced transformation of fossil mastodon ivory into turquoise 'odontolite'. Structural and elemental characterisation. Solid State Sci, 2000; 2(6): 625–636.
14. Müller K, Reiche I. Differentiation of archaeological ivory and bone materials by micro-PIXE/PIGE with emphasis on two upper Palaeolithic key sites: Abri Pataud and Isturitz, France. J Archaeol Sci. 2011;38(12):3234–43.
15. Locke M. Structure of ivory. J Morphol. 2008;269:423–50.
16. Solov'Ev TM, Petukhova ES, Botvin GV, Isakova TA, Pavlova VV. Analyzing the composition and structure ofmammuthus primigeniustusk by methods of thermogravimetric and x-ray analysis. Inorg Mater Appl Res. 2021; 12(4): 1083–1086.
17. Piga G, Gonçalves D, Thompson TJU, Brunetti A, Malgosa A, Enzo S. Understanding the crystallinity indices behavior of burned bones and teeth by ATR-IR and XRD in the presence of bioapatite mixed with other phosphate and carbonate phases. Int J Spectr. 2016;2016:4810149.
18. Piga G, Solinas G, Thompson TJU, Brunetti A, Malgosa A, Enzo S. Is X-ray diffraction able to distinguish between animal and human bones. J Archaeol Sci. 2013; 40(1): 778–785.
19. Bigi A, Falini G, Foresti E, et al. Magnesium influence on hydroxyapatite crystallization. J Inorg Biochem. 1993;49(1):69–78.
20. Weiner S, Bar-Yosef O. States of preservation of bones from prehistoric sites in the Near East: a survey. J Archaeol Sci. 1990; 17: 187–196.
21. Rey C, Shimizu M, Collins B, Glimcher MJ. Resolution-enhanced Fourier transform infrared spectroscopy study of the environment of phosphate ion in the early deposits of a solid phase of calcium phosphate in bone and enamel and their evolution with age: I. Investigations in the ν_4 PO_4 domain. Calcif Tissue Int. 1990;46(6):384–94.
22. Daveri A, Malagodi M, Vagnini M. The bone black pigment identification by noninvasive, in situ infrared reflection spectroscopy. J Anal Methods Chem. 2018;2018:6595643.
23. Habelitz S, Pascual L, Durán A. Transformation of tricalcium phosphate into apatite by ammonia treatment, J Mater Sci. 2001; 36: 4131–4135,
24. Jang HL, Jin K, Lee J, Kim Y, Nahm SH, Hong KS, et al. Revisiting whitlockite, the second most abundant biomineral in bone: nanocrystal synthesis in physiologically relevant conditions and biocompatibility evaluation. ACS Nano. 2014;8(1):634–41.
25. Tavares DS, Castro LO, Soares GDA, et al. Synthesis and cytotoxicity evaluation of granular magnesium substituted-tricalcium phosphate. J Appl Oral Sci. 2013;21:37–42.
26. Li X, Ito A, Sogo Y, Wang X, Legeros RZ. Solubility of mg-containing β-tricalcium phosphate at 25 °C. Acta Biomater. 2009;5(1):508–17.
27. Rey C, Shimizu M, Collins B, Glimcher MJ. Resolution-enhanced Fourier transform infrared spectroscopy study of the environment of phosphate ion in the early deposits of a solid phase of calcium phosphate in bone and enamel and their evolution with age: II. Investigations in the ν_3 PO_4 domain. Calcif Tissue Int. 1991; 49: 383–388.
28. Butler DH, Shahack-Gross R. Formation of biphasic hydroxylapatite-beta magnesium tricalcium phosphate in heat treated salmonid vertebrae. Sci Rep. 2017; 7(1): 3610.
29. Hamada M, Nagai T, Kai N, Tanoue Y, Mae H, Hashimoto M, et al. Inorganic constituents of bone of fish. Fish Sci. 2008;61(3):517–20.
30. Mkukuma L D, Skakle J, Gibson IR, Imrie CT, Aspden RM, Hukins D. Effect of the proportion of organic material in bone on thermal decomposition of bone mineral: an investigation of a variety of bones from different species using thermogravimetric analysis coupled to mass spectrometry, high-temperature x-ray diffraction. Calcif Tissue Int. 2004; 75(4): 321–328.
31. Fadeev IV, Shvorneva LI, Barinov SM, Orlovskii VP. Synthesis and structure of magnesium-substituted hydroxyapatite. Inorg Mater. 2003; 39(9): 947–950.
32. Reiche I, Heckel C, Müller K, Jöris O, Matthies T, Conard NJ, Floss H, White R. Combined non-invasive PIXE/PIGE analyses of mammoth ivory from Aurignacian archaeological sites. Angew Chem Int Ed. 2018;57(25):7428–32.
33. Heckel C, Müller K, White R, Wolf S, Conard NJ, Normand C, Floss H, Reiche I. F-content variation in mammoth ivory from Aurignacian contexts: preservation, alteration, and implications for ivory-procurement strategies. Quatern Int. 2016;403:40–50.
34. Heckel C, Müller K, White R, Floss H, Conard NJ, Reiche I. Micro-PIXE/PIGE analysis of Palaeolithic mammoth ivory: potential chemical markers of provenance and relative dating. Palaeogeogr Palaeoclimat Palaeoecol. 2014;416:133–41.

Publisher's Note